DRUG DELIVERY
2023, VOL. 30, NO. 1, 2162626
https://doi.org/10.1080/10717544.2022.2162626

Taylor & Francis
Taylor & Francis Group

RESEARCH ARTICLE

OPEN ACCESS Check for updates

In-depth study of anticancer drug diffusion through a cross-linked pH-responsive polymeric vesicle membrane

Fen Zhang[a], Qian Yao[a], Xiaoqi Chen[a], Haijun Zhou[a], Mengmeng Zhou[a], Yantao Li[a] and Hua Cheng[b]

[a]Institute of Energy Resources, Hebei Academy of Sciences, Shijiazhuang, Hebei Province, China; [b]Institute of Biology, Hebei Academy of Sciences, Shijiazhuang, Hebei Province, China

ABSTRACT

Post-encapsulation and release of the anticancer drug doxorubicin hydrochloride (DOX·HCl) through cell-like transmission functions of polymeric vesicles were studied using cross-linked pH-responsive polymeric vesicles. The vesicles were fabricated for the first time via the redox-initiated reversible addition-fragmentation chain transfer dispersion polymerization in ethanol-water mixture, using 2-(diisopropylamino)ethyl methacrylate and glycidyl methacrylate, and the vesicle membrane was modified post-cross-linking by using ethylenediamine. A phase diagram was constructed for reproducible fabrication of the polymeric vesicles, and well-shaped vesicles were formed when the target degree of polymerization of the hydrophobic polymer chains was equal to or higher than 50 with solid content in the range of 10–30 wt%. The cross-linked vesicle membrane served as a gate enabling "open" and "closed" states in response to pH stimulation. Up to 50% drug loading efficiency and 39% drug loading content could be achieved, and in vitro release of the DOX-loaded vesicles in aqueous buffer solutions showed a much faster DOX release rate at pH 5.0 than at pH 6.5. The polymeric vesicles were of very low cytotoxicity to A549 cells up to the concentration of 2 mg/mL, and the IC_{50} of DOX-loaded vesicles were higher than that of the free DOX. The intracellular DOX release study indicated higher cellular uptake capability for DOX-loaded vesicles than that of free DOX.

ARTICLE HISTORY
Received 4 August 2022
Revised 17 September 2022
Accepted 18 September 2022

KEYWORDS
pH-responsive; polymeric vesicles; redox-initiated; RAFT dispersion polymerization; anticancer drug delivery

1. Introduction

Cancer has become one of the most serious diseases threatening human life in recent years, and chemotherapy is the most commonly used treatment method, however, due to the severe side effects, poor stability and water solubility of the therapeutic drugs (Lee & Feijen, 2012; Hu et al., 2013; Zhang et al., 2016; Tenchov et al., 2021), polymeric drug delivery carriers, which could potentially reduce the unexpected side effects, increase drug circulation time, improve drug solubility, and also make the targeted drug delivery possible (Peer et al., 2007; Fox et al., 2009; Liu et al., 2009; Hu et al., 2017; Tenchov et al., 2021), have emerged and got more and more attention. For better realization of drug delivery, the design of controlled-release polymeric drug delivery carriers has evolved, especially the stimuli-responsive polymeric drug delivery carriers that exploit local biochemical changes (such as changes in pH, redox state, enzymatic activity, and ionic content) at the disease positions to trigger drug release (Kamaly et al., 2016).

Several drug delivery carriers, such as polymers, polymeric micelles, nanoparticles, liposome, and polymeric vesicles, have been developed as the drug reservoir for therapeutic treatments. Among them, polymeric vesicles have received more and more attention because of their good designability and stability, internal and external hydrophilic properties, and the hydrophobicity of the membrane core, which makes them useful as medical carriers for hydrophobic, hydrophilic, and amphiphilic therapeutics, such as anticancer drugs (Chen et al., 2010; Karagoz et al., 2014; Qiu et al., 2016), nucleic acid drugs (Lomas et al., 2007; Kim et al., 2019), and functional enzymes (Liu et al., 2017; Moreno et al., 2021). A wide variety of responsive modalities has been incorporated into the building blocks for the design of smart polymeric vesicles to combat disease (Colley et al., 2014; Feng & Yuan, 2014; Wang et al., 2015; Che & van Hest, 2016; Thambi et al., 2016; Yao et al., 2020; Sztandera et al., 2022). pH-responsive chimeric polymeric vesicles decorated with 2-[3-[5-amino-1-carboxypentyl]-ureido]-pentanedioic acid (Acupa) had been formed for drug delivery application, and could efficiently deliver therapeutic proteins into prostate cancer cells (Li et al., 2015). CO_2-responsive polymeric vesicles were synthesized by introducing 2-(dimethylamino)ethyl methacrylate (DMAEMA) into the core-forming block, and bovine serum albumin (BSA) was encapsulated and released via a CO_2-trigger under mild conditions (Tan et al., 2017). In addition, cross-linking of vesicle membrane endows them with good structural

CONTACT Fen Zhang fen.zhang1105@hotmail.com; Yantao Li 13903116163@163.com Institute of Energy Resources, Hebei Academy of Sciences, Shijiazhuang, Hebei Province 050081, China; Hua Cheng cheng_hua@sina.com Institute of Biology, Hebei Academy of Sciences, Shijiazhuang, Hebei Province 050081, China

stability and permeability property. Polyprodrug-gated cross-linked vesicles poly(ethylene glycol)-b-p(camptothecin prodrug monomer-co-3-(trimethoxysilyl)propyl methacrylate) were fabricated and concomitant release of hydrophobic and hydrophilic drugs could be achieved through reduction-sensitive modulation of bilayer permeability (Hu et al., 2018). The concurrent cross-linking and permeabilizing of pH-responsive polymeric vesicles containing Schiff base moieties via enzyme-catalyzed acid production were reported, and the permeabilization of the vesicles could be regulated through pH gradient to realize the controlled release (Liu et al., 2022). The formulation of polymeric nano-objects by using the photosensitive monomers 2-nitrobenzyl methacrylate (NBMA) and 7-(2-methacryloyloxy-ethoxy)-4-methyl-coumarin (CMA) was reported (Zhang et al., 2017), and after post-polymerization photo-irradiation, the produced vesicles were endowed with pH-responsive performance and robust structures, which exhibited excellent performance in drug delivery studies.

For the preparation of polymeric vesicles, self-assembly of block copolymers via post-polymerization processing steps is the conventionally-used method, but the lower solid content (typically less than 1%) and the complicated preparation process have limited its application. Reversible addition-fragmentation chain transfer (RAFT)-mediated dispersion polymerization is a one-pot polymerization strategy for the production of polymeric vesicles at much higher concentration with numerous monomers, which makes it potentially scalable (Gao et al., 2014; Zhang et al., 2017). During the past several years, various RAFT techniques have been developed, such as thermal-initiated RAFT polymerization (Warren & Armes, 2014; Zhu et al., 2017), redox-initiated RAFT polymerization (Deane et al., 2020; Park et al., 2020), photo-induced RAFT polymerization (Du et al., 2021), metal-catalytic initiation (Gu et al., 2014; 2015), polyethylene-terephthalate-RAFT (PET-RAFT) polymerization (Tian et al., 2018), and enzyme-catalysis-mediated (Enz) RAFT polymerization (Liu et al., 2017; Lv et al., 2017). When compared with thermal, light, metal, PET, and enzyme-catalysis initiated polymerization, redox-initiated polymerization could proceed under relatively lower temperatures and has been widely used in many industrial products. In the redox-initiated RAFT polymerization, the low reaction temperature could reduce the possibility of side reactions, resulting in high conversion and low dispersity. Poly(n-butyl acrylate) nanoparticles were produced via the RAFT aqueous emulsion polymerization of n-butyl acrylate (nBA) with potassium persulfate (KPS)/ascorbic acid as the initiator at a polymerization temperature of 30 °C (Deane et al., 2020). Dispersion polymerization of 2-methoxyethyl acrylate (MEA) was done in water to produce nanoparticles using the redox initiator KPS/sodium ascorbate, and high efficiency was found at low polymerization temperatures of 30 or 40 °C (Liu et al., 2011). Redox-initiated RAFT-mediated emulsion polymerization of glycidyl methacrylate (GlyMA) was conducted by using poly(ethylene glycol) methyl ether methacrylate-4-cyano-4-(dodecylsulfanylthiocarbonyl) sulfanylpentanoic acid (PEGMAn-CDPA-Me) as a macro-RAFT agent, and a range of morphologies, including spheres, worms, and vesicles, were prepared (Dai et al., 2019). However, to the best of our knowledge, there have been no reports on the synthesis of pure polymeric vesicles with redox initiation via RAFT polymerization in a non-aqueous solvent.

Herein, we reported the preparation of polymeric vesicles via RAFT dispersion polymerization with the redox initiator KPS/sodium bisulfite (SBS) in an ethanol-water solvent. Poly(ethylene oxide)-4-(4-cyanopentanoic acid) dithiobenzoate (mPEG-CPADB) was synthesized and used as a macro chain transfer agent, and 2-(diisopropylamino)ethyl methacrylate (DIPEMA) and GlyMA were used as monomers for the preparation of pH-responsive polymeric vesicles. The obtained polymeric vesicles were further cross-linked by using ethylenediamine (EDA), which endowed the membrane of the vesicles with "open" and "closed" states by adjusting the pH value. For the implementation of cell-like functions within vesicles, post-encapsulation with doxorubicin hydrochloride (DOX·HCl, an anthracycline-based broad-spectrum anticancer drug (Li et al., 2022)), was performed without changing the morphology of the vesicles, and the in vitro release of the DOX-loaded vesicles in aqueous buffer solutions was evaluated (Scheme 1). The cytotoxicity of the polymeric vesicles, free DOX and DOX-loaded vesicles to non-small cell lung carcinoma A549 cells and the intracellular drug delivery were also investigated.

2. Materials and methods

2.1. Materials

The α-methoxy-ω-hydroxypoly(ethylene oxide) (mPEG, number average molecular weight (Mn) = 1900), DOX·HCl, CPADB, 4-(dimethylamino)pyridine, and dicyclohexylcarbodiimide were purchased from Aladdin and used as received. DIPEMA (97%) and GlyMA were purchased from Aladdin and purified by passing the compounds through a column of Al_2O_3 to remove inhibitors. KPS (United Initiators (Shanghai) Co., Ltd.), SBS (Damao Chemical Reagent Factory), and 2-(4-amidinophenyl)-6-indolecarbamidine dihydrochloride (DAPI, Solarbio) were purchased and used without further purification. Other chemicals were of analytical grade and used as received.

2.2. Preparation of polymeric vesicles with cross-linked membrane

For the preparation of the polymeric vesicles, redox-initiated RAFT dispersion polymerization was applied. The macro-RAFT agent, mPEG-CPADB, was synthesized by an esterification reaction in anhydrous dichloromethane at room temperature using CPADB as the RAFT agent (Zhang et al., 2021). A typical protocol was performed as followed. First, DIPEMA (0.3413 g, 1.6000 mmol), GlyMA (0.0569 g, 0.4000 mmol), mPEG-CPADB (0.0440 g, 0.0200 mmol), KPS (0.0014 g, 0.0050 mmol), SBS (0.0005 g, 0.0050 mmol), and a solvent (2.5166 g, with a mass ratio of ethanol-water = 6:4) were added into a glass tube with a magnetic bar. The oxygen was removed from the reaction mixture by three pump-N_2 purge cycles before sealing the glass tube, and then put it in the oven at 35 °C with

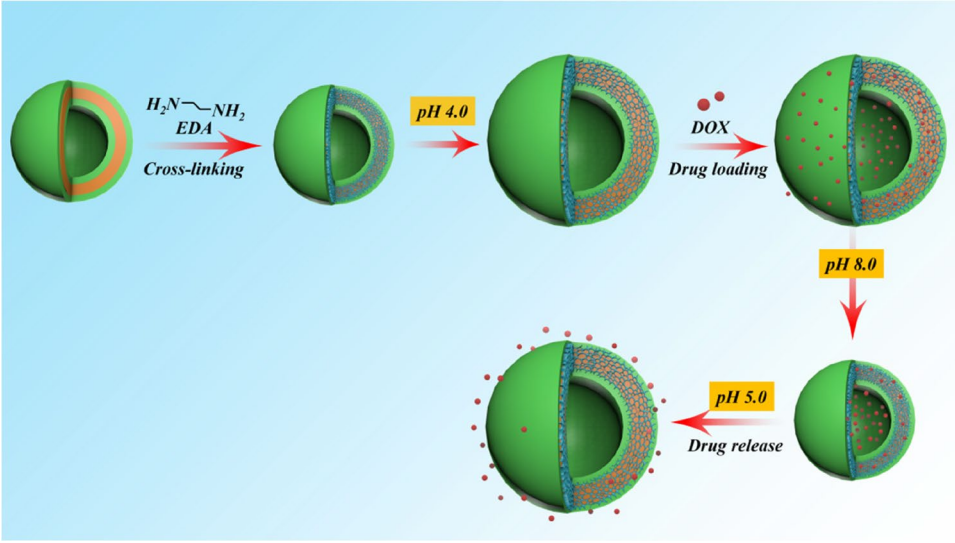

Scheme 1. "Open" and "closed" cycles of the membrane of the vesicles in response to pH stimuli.

magnetic stirring for 7 h. The reaction mixture was put into cold water to be quickly cooled and then opened to air to quench the polymerization.

The cross-linking of the mPEG-P(DIPEMA-co-GlyMA) vesicle membrane was done as followed. 0.2000 g of the produced samples were diluted 20-fold with the reaction solvent, and then ethylenediamine (EDA; 0.0017 g, 0.0270 mmol, EDA/GlyMA molar ratio = 1:1) was added. The reaction was proceeded for 24 h under stirring at 24 °C, and then the unreacted EDA was removed through centrifugation-redispersion cycles.

2.3. Encapsulation of DOX into the vesicles

The cross-linked vesicles (0.01 g) after purification were dispersed in an acid buffer solution (pH 3.0, 4.0 or 5.0 buffer solution, 4 mL), and then DOX·HCl (5.0 mg) was added to the dispersion. The mixture was stirred at room temperature for one day in the dark, and then NaOH aqueous solution (0.2 M) was used to adjust its pH to about 8.0. The unencapsulated DOX was removed by dialysis (molecular weight cutoff of the dialysis tube, 3500 Da) against a phosphate-buffered saline (PBS) solution (pH 7.4, 0.02 M) with regular exchanges of the solution with fresh PBS until no more DOX could be detected in the solution outside the dialysis tube. The drug loading efficiency (LE) and drug loading content (LC) of the vesicles were determined by using an ultraviolet-visible (UV-Vis) spectroscopy quantitative method to determine the amount of drug dialyzed into the PBS solution, which could be used to calculate the amount of DOX encapsulated, and a standard curve was acquired by plotting the UV absorbance at 480 nm against the DOX concentration in the PBS solution. LE and LC were calculated according to equations (1) and (2), respectively, as:

$$\mathrm{LE}(\%) = \frac{\text{weight of DOX encapsulated in the vesicles}}{\text{weight of the DOX in feed}} \times 100\% \quad (1)$$

$$\mathrm{LC}(\%) = \frac{\text{weight of DOX encapsulated in the vesicles}}{\text{weight of the vesicles}} \times 100\% \quad (2)$$

2.4. In vitro pH-regulated drug release

For investigation of the DOX release efficiency from the DOX-loaded vesicles, different pH conditions (pH = 5.0 and 6.5) were studied. 1.5 mL of the above prepared DOX-loaded vesicle solution was added to a dialysis tube (molecular weight cutoff of 3500 Da), and then put in a weighing bottle, followed by the addition of 40 mL of buffer solution with pH = 5.0 or 6.5. The weighing bottle was kept at 37 °C on a shaking bed with rotational speed of 200 rpm. At selected time points, 3 mL of the dialysis solution was removed for measurement of the released DOX, while an equal volume of fresh buffer solution was added to the bottle. UV standard curves of DOX in pH = 5.0 and 6.5 buffer solutions were generated as above in PBS solution, which were used for the evaluation of the selected samples at different dialysis times, and then the DOX releasing curves were acquired. To minimize the experimental error, each test was done in duplicate, and the mean value was recorded.

2.5. In vitro cytotoxicity evaluation

A549 cells were chosen for evaluating the in vitro cytotoxicity using a Cell Counting Kit-8 (CCK-8) assay. The cells were first cultured in Dulbecco's modified Eagle's medium/nutrient mixture F-12 Ham (DMEM/F-12 1:1) supplemented with 10% FBS at 37 °C in a CO_2/air (5:95) incubator. For CCK-8 assay, 96-well plates were used for the cell incubation, and each well was seeded with 5000 A549 cells. After incubating for one day, different concentrations of either DOX·HCl solution, the cross-linked vesicle solution, or the DOX-loaded vesicle solution were added to the wells and incubated for another 24 h. Then the culture medium was taken out and added with 100 µL of 10% CCK-8 solution and incubated for 2 h at 37 °C.

Thermo 1510 instrument was applied to measure the absorbance values of the samples at a wavelength of 450 nm, and $[(A_s\text{-}A_b)/(A_c\text{-}A_b)] \times 100\%$ was used for the cell viability calculation, where A_s and A_c are the absorbance values with and without the addition of the vesicles (with or without DOX), respectively, and A_b is the absorbance value of the plain medium. Each test was done in duplicate, and the mean value was recorded.

2.6. Intracellular drug delivery

A549 cells were cultured in DMEM/F-12 1:1 supplemented with 10% FBS in a 4-well plate under an atmosphere of 5% CO_2 at 37 °C for 5 h, and the culture medium was refreshed with DMEM/F-12 with the free DOX solution or the DOX-loaded vesicle solution, equivalent to a 0.2 μg/mL concentration of DOX. The culture medium was taken out and the cells were washed with PBS two times after culturing for 24 h, and then formaldehyde was added to fix the cells for 0.5 h at room temperature. After removal of the formaldehyde, the cells were washed with PBS two times and then stained with DAPI. After washing with PBS three times, the cells were observed with a confocal laser scanning microscope (CLSM) (Leica TCs SP8) at 488 nm and 595 nm (Ex = 405 nm and 488 nm).

2.7. Characterization

The morphologies of the nanoparticles were measured with transmission electron microscopy (TEM, JEM-2100 Plus electron microscope) at an accelerating voltage of 200 kV. The samples were dispersed in ethanol-water or buffer solution and then deposited on copper grids, and then stained with phosphotungstic acid before characterization. The ^{1}H NMR spectra were carried out on a Bruker DMX500 spectrometer, and $CDCl_3$ was used as the solvent and tetramethylsilane was used as an internal reference. Hydrodynamic diameter and zeta potential measurements were done on a dynamic light scattering (DLS) spectrometer (PPS Z3000, Particle Sizing Systems, UK). The acid-base titration was carried out on a ZDJ-4B automatic potentiometric titrator. The Fourier transform infrared (FTIR) spectroscopy was performed on a PerkinElmer Frontier FTIR spectrometer. UV-vis measurements were carried out on a TU-1901 UV-vis spectrophotometer. CLSM images were recorded on a Leica TCS SP8 microscope.

3. Results and discussion

3.1. Fabrication of vesicles via redox-initiated RAFT dispersion copolymerization of DIPEMA and GlyMA

Redox-initiated RAFT dispersion polymerization was done in ethanol-water solvent by using DIPEMA and GlyMA for the fabrication of pH-responsive polymeric vesicles, and water soluble KPS/SBS were used as the redox initiator. The results of thermal-initiated RAFT dispersion copolymerization of DIPEMA and GlyMA in a previous study (Zhang et al., 2021) showed the formation of well-shaped mPEG-P(DIPEMA-co-GlyMA) vesicles with a large space on the phase diagram, and the produced vesicles showed clear pH responsiveness after cross-linking of the vesicle membrane. To better understand this redox-initiated polymerization system, a phase diagram was also constructed to identify the conditions for the production of pure vesicles. mPEG-CPADB (Mn = 2500 and Mw/Mn = 1.18) was synthesized by the esterification reaction of mPEG and CPADB in anhydrous dichloromethane at room temperature and then used as the macro-RAFT agent in the following RAFT dispersion copolymerization. A lower polymerization temperature of 35 °C was used due to the lower activation energy and higher radical generation rate of the redox initiation. The solid content and the target degree of polymerization (DP) of the P(DIPEMA-co-GlyMA) block, which were the two main factors affecting the nanoparticle morphologies, were used for the generation of the phase diagram, as shown in Figure 1. With solids content in range of 10 to 30%, only spheres and vesicles could be fabricated, and at each value of the solids content, with the increasing of target DP, similar morphological transition was found, from spheres to vesicles, and along with the two mixed phases. When the target DP of P(DIPEMA-co-GlyMA) ≥ 50, pure polymeric vesicles could be obtained, which indicated that vesicles could be produced in a wide space in this polymerization system. Similar to the previous study of azobisisobutyronitrile (AIBN)-initiated RAFT dispersion copolymerization of DIPEMA and GlyMA (Zhang et al., 2021), relatively lower target DP was needed for the polymeric vesicles preparation in this redox-initiated polymerization system, while DP was generally ≥ 80 for methacrylate monomers in other RAFT dispersion polymerization systems to fabricate vesicles (Penfold et al., 2019; Xu et al., 2019).

3.2. Evaluation of vesicles with cross-linked membrane

For the preparation of polymeric vesicles with permeable membranes, cross-linking of the mPEG-P(DIPEMA-co-GlyMA) vesicle membrane was performed by using EDA to react with the epoxy functional groups on the vesicles in an ethanol-water mixture. After the cross-linking reaction, the produced samples were further purified via the centrifugation-redispersion cycles. ^{1}H NMR was applied to characterize the chemical structure of the mPEG-P(DIPEMA-co-GlyMA) vesicles produced via the redox-initiated polymerization system, as shown in Figure 2(a), and obvious epoxy group signals were found (peaks at δ 3.2 (c), δ 2.63, and 2.82 (d)). And the reaction between the epoxy groups and EDA was confirmed by FTIR spectroscopy, as shown in Figure 2(b) for the FTIR spectra, after the reaction the absorption peak of the epoxy group at 842 cm^{-1} became much weaker.

The tertiary amine groups in the PDIPEMA block could be protonated under acid condition (pKa is approximately 6.3 (Bories-Azeau et al., 2004)), and the degree of the protonation of the PDIPEMA block on the cross-linked vesicles was studied by using the acid-base titration method at pH 3.0, 4.0, 5.0, 6.0 and 7.0 conditions. The cross-linked vesicles were first dispersed in deionized water and titrated with

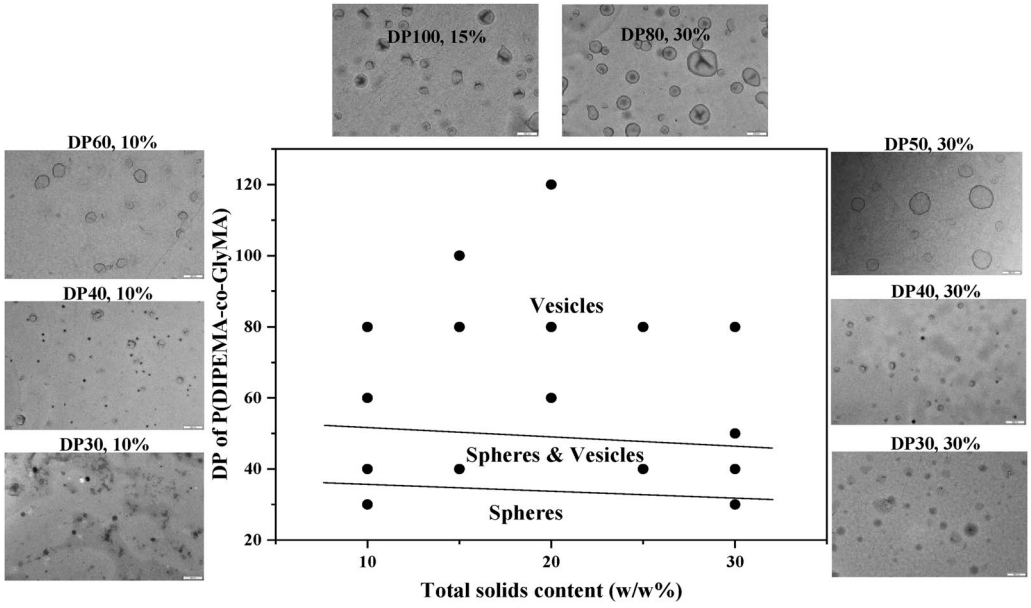

Figure 1. Phase diagram generated by varying the target DP of P(DIPEMA-co-GlyMA) and the solid content.

hydrochloric acid to the pre-set pH value, and then sodium hydroxide was used for titration to determine the end points. The degree of protonation of the PDIPEMA block decreased with the increasing of pH value of the dispersion solution, and was higher than 60% when pH value was equal to or lower than 5.0, as shown in Figure 2(c).

To check the stability of the cross-linked vesicles in acid buffer solutions, the cross-linked vesicles were redispersed in pH 7.4 PBS solution, pH 5.0, pH 4.0 and pH 3.0 buffer solutions, and the TEM images, zeta potential, and hydrodynamic diameter and its distribution index (PDI) were studied. Seen from Figure 2(e)–(h), clear and thin vesicle membranes could be observed in pH 7.4 PBS solution, while the vesicle membrane became more and more thicker and unclear as the decreasing of the solution pH value, which was consistent with the Eisenberg group result on the vesicle wall structure at different pH values for poly(ethylene oxide)-b-polystyrene-b-poly(2-diethylaminoethyl methacrylate) vesicles (Yu et al., 2009). The cross-linked vesicles were swollen at the acid conditions for the protonation of the tertiary amine groups in the PDIPEMA block, while their morphologies could be maintained. The hydrodynamic diameter of the vesicles in different buffer solutions was also evaluated by DLS, and it showed a significant increase from about 195 nm in pH 7.4 PBS solution to about 380 nm in pH 3.0 buffer solution, while the PDI kept in range of 0.10–0.14, as shown in Figure 2(d), and the zeta potential showed a little decrease as the increasing of the solution pH value. For the non-cross-linked mPEG-P(DIPEMA-co-GlyMA) vesicles, when dispersed in pH 4.0 buffer solution, transparent solution would be obtained and no vesicle could be observed on the TEM photo (Figure 2(i)). This indicated that cross-linking of the vesicle membrane increased the structural stability of the vesicles in an acid environment, which made it a possible candidate to utilize the pH responsibility of the cross-linked vesicles for encapsulation and release of the drugs.

3.3. Encapsulation of DOX

For the general drug encapsulation method, the formation of the nanoparticles and encapsulation of the drugs were done at the same time, which was to mix the drugs and block copolymers together in organic solvents, and after addition of a non-solvent into the mixture, the drugs were encapsulated accordingly during the nanoparticle formation process (Zhu et al., 2013; Zhang et al., 2017). Herein, the vesicles with cross-linked membrane were pre-prepared, and the anticancer drug DOX was loaded into the vesicles by mixing DOX·HCl and the cross-linked vesicles in an acid buffer solution (in which the pores in the vesicle membrane would open for the protonation of the tertiary amine groups in PDIPEMA block), and after stirring for 24 h, the pH of the solution was adjusted to approximately 8.0 to close the pores in the vesicle membrane and encapsulate DOX inside the vesicles, as illustrated in Scheme 1.

For this post-encapsulation method, the DOX was encapsulated into the vesicles through the pores of the vesicle membrane under acidic environment, and the hydrogen bond interaction between the cross-linked vesicle membrane P(DIPEMA-co-GlyMA) and DOX also helped DOX to enter the vesicles. The produced DOX-loaded vesicles were dialyzed in PBS (pH = 7.4) to completely remove the unencapsulated DOX. Figure 3(a) shows the UV curves of the vesicles, DOX·HCl, and the DOX-loaded vesicles, and the DOX characteristic peak in the range of 420–550 nm was clearly observed for the DOX-loaded vesicles. Figure 3(b)–(d) shows the TEM morphology of the DOX-loaded vesicles prepared in pH 3.0, 4.0 and 5.0 buffer solutions, and the vesicle morphology could be maintained after DOX encapsulation.

To calculate the drug loading efficiency (LE) and drug loading content (LC) in the vesicles, a UV-vis quantitative method was used. A standard curve was made by plotting the UV absorbance at 480 nm against the concentration of DOX, and the regression curve $y = 0.01792x - 0.00162$ with

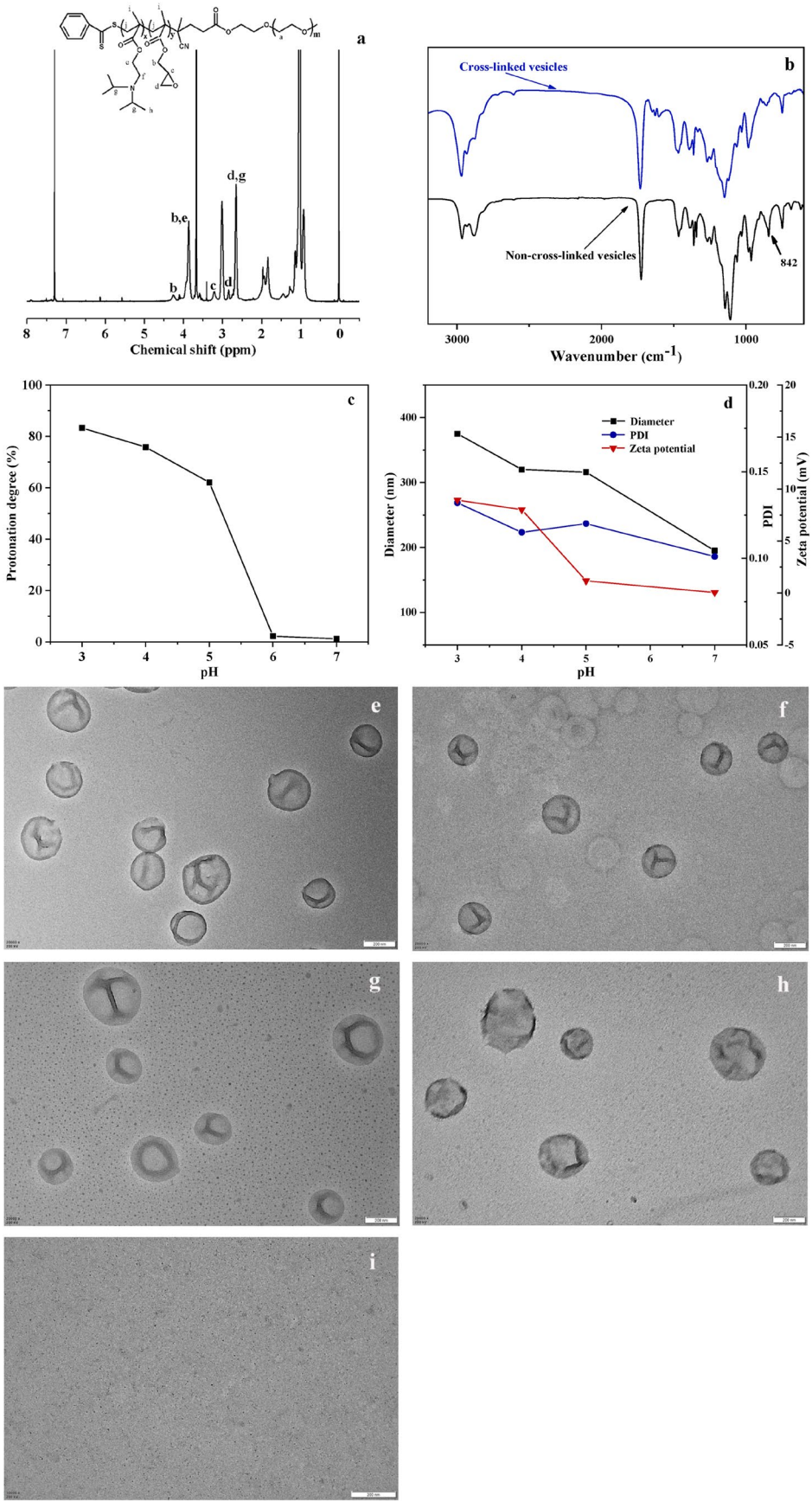

Figure 2. (a) ^{1}H NMR spectra of mPEG-P(DIPEMA-co-GlyMA) vesicles; (b) FTIR spectra of mPEG-P(DIPEMA-co-GlyMA) vesicles before and after reacting with EDA; (c) the degree of the protonation of the PDIPEMA block vs. pH value of the dispersion solution; (d) hydrodynamic diameter, PDI and zeta potential of the vesicles measured in pH 7.4 PBS solution, pH 5.0, pH 4.0 and pH 3.0 buffer solutions by using DLS; (e-h) TEM images of cross-linked mPEG-P(DIPEMA-co-GlyMA) vesicles dispersed in pH 7.4 PBS solution, pH 5.0, pH 4.0 and pH 3.0 buffer solutions respectively; and (i) TEM image of non-cross-linked mPEG-P(DIPEMA-co-GlyMA) vesicles dispersed in the pH 4.0 buffer solution.

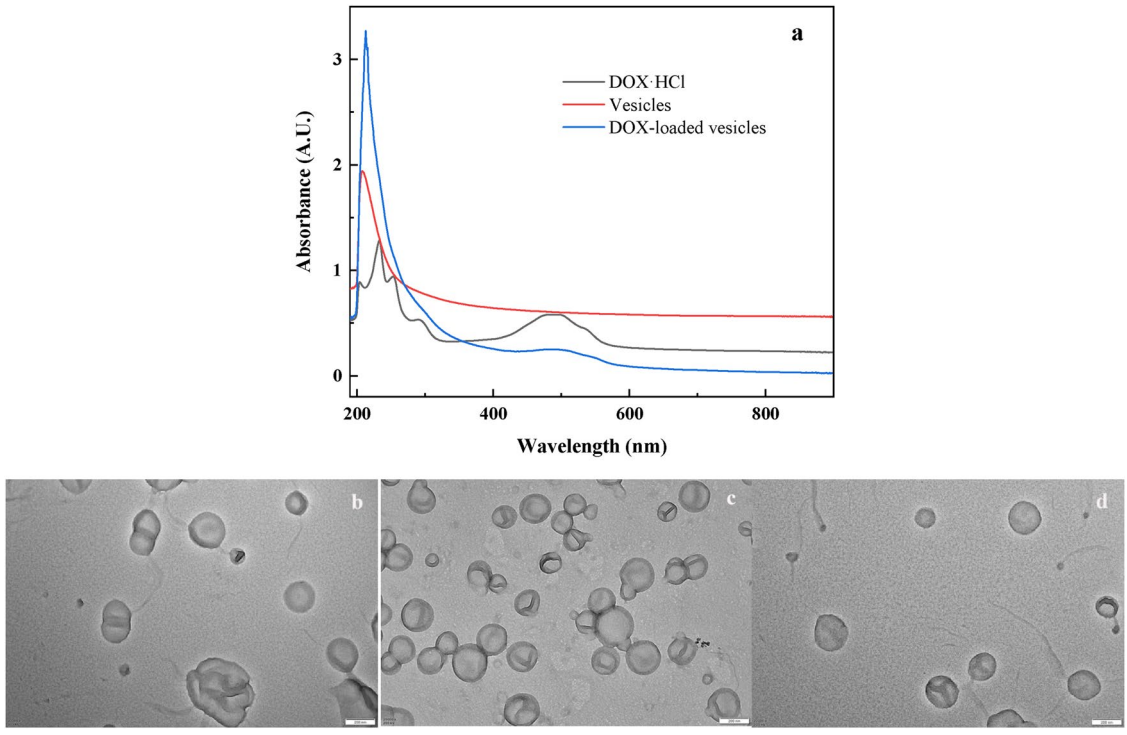

Figure 3. (a) UV curves of vesicles, DOX·HCl, and the DOX-loaded vesicles; and (b-d) TEM images of the DOX-loaded vesicles prepared in pH 3.0, pH 4.0 and pH 5.0 buffer solutions respectively.

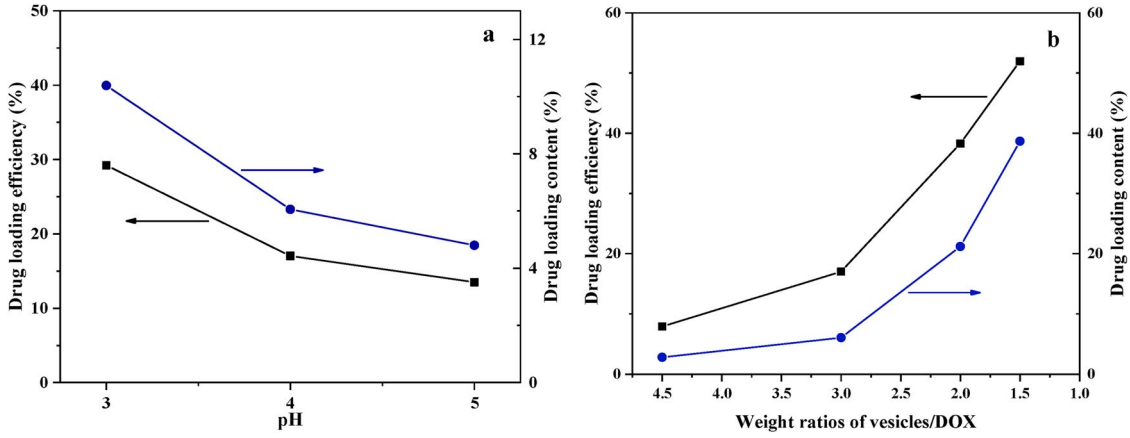

Figure 4. (a) Drug loading efficiency (LE) and drug loading content (LC) values vs. pH value of the buffer solutions; (b) drug loading efficiency (LE) and drug loading content (LC) values vs. weight ratios of vesicles/DOX.

R^2 = 0.9996 was obtained for the DOX concentration. LE and LC of the DOX-loaded vesicles done in pH 3.0, 4.0 and 5.0 buffer solutions were shown in Figure 4(a), and both LE and LC decreased as the increasing of the pH value of the buffer solution used for drug encapsulation, which indicated that the lower the pH value, the better the membrane permeability of the cross-linked vesicles. The effect of weight ratios of vesicles/DOX on LE and LC were also studied in pH 4.0 buffer solution. As shown in Figure 4(b), both LE and LC increased as the DOX loading ratio increased, and as high as 50% LE and 39% LC could be achieved with vesicles/DOX at 1.5:1. Further increasing the DOX loading ratio caused instability of the vesicle solution after adjusting solution pH to 8.0, which might be caused by the poor solubility of DOX in the solution. The successful encapsulation of DOX into the vesicles indicated that vesicles with cross-linked membranes have certain permeability and could be potentially used for drug encapsulation.

3.4. In vitro release of DOX

As mentioned previously in the introduction, for the protonation of the tertiary amine groups on PDIPEMA chains in acid conditions, the pores in the vesicle membrane would open and the DOX in the DOX-loaded vesicles can be released under the acidic environment (as illustrated in Scheme 1). For the in vitro release study of the DOX-loaded vesicles (prepared with a weight ratio of vesicles: DOX = 2:1 in pH 4.0 buffer solution), buffer solutions of pH = 6.5 and

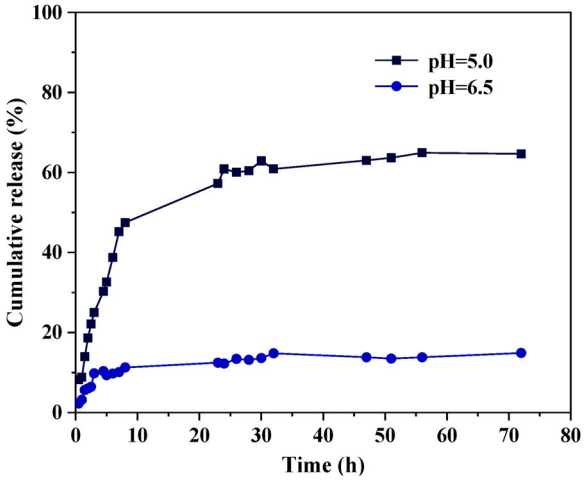

Figure 5. DOX release profiles of the DOX-loaded vesicles in the aqueous buffer solutions at pH = 6.5 and at pH = 5.0 (cumulative release (%) vs. time (h)).

5.0 (microenvironment of tumor approximately pH = 6.5, and tumor cell approximately pH = 5.0–5.5 (Yu et al., 2020)) were used as the dialysis solution to simulate the tumor environment, and the results are shown in Figure 5. When the drug release test was carried out at pH = 6.5, about 12% of the DOX in the vesicles was released within the first 24 h, and then the release amount did not change much, and only increased to about 15% after 72 h; while in pH = 5.0 buffer solution, a much more rapid release of DOX from the vesicles could be observed, as shown in Figure 5. Up to 47% of DOX was released within the first 8 h, and reached as high as 65% after 72 h, which was owing to the protonation of the tertiary amine groups in the more acidic solution, and thus making the pores in the vesicle membrane open for easy release of the drug. The result was consistent with reported result for the pH-responsive release of the polymeric nano-objects made by NBMA and CMA (Zhang et al., 2017), and a much faster drug release speed at pH

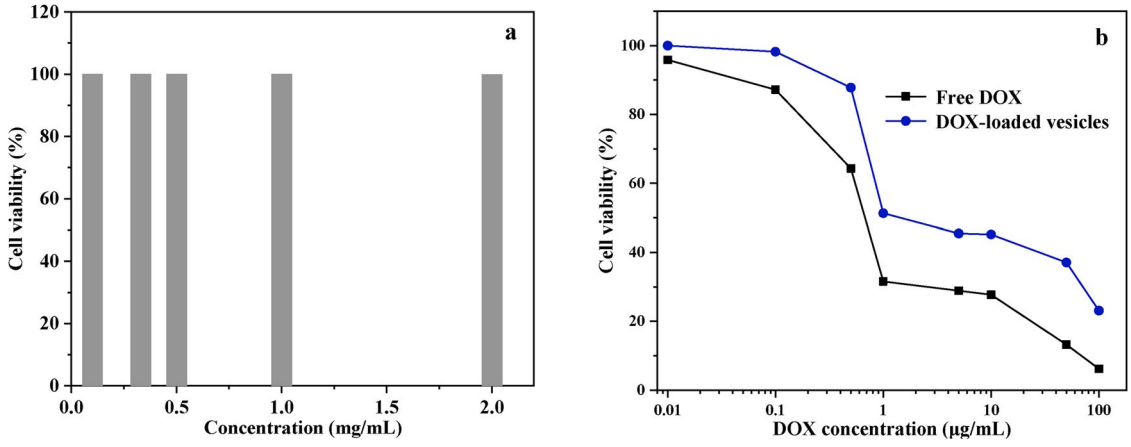

Figure 6. (a) Cell viability vs. different concentrations of cross-linked vesicles; and (b) cell viability vs. different concentrations of free DOX and the DOX-loaded vesicles.

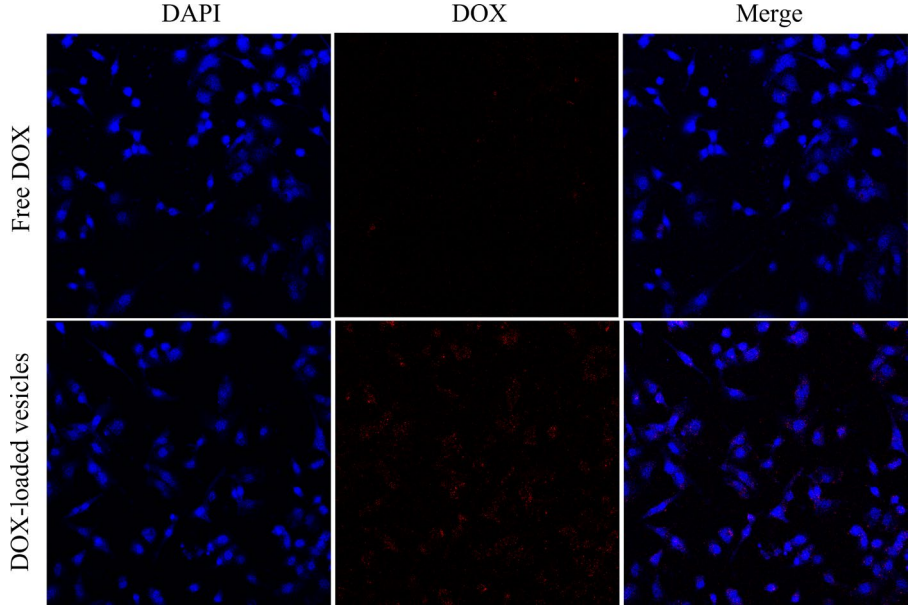

Figure 7. Confocal laser scanning microscope images of the A549 cells treated with free DOX solution and the DOX-loaded vesicle solution at 37 °C for 24 h and stained with DAPI. The images from left to right display DAPI (blue), DOX (red), and a merge of the two images.

5.4 than in a pH-neutral environment for the DOX-loaded nano-objects. The pH responsibility of the cross-linked vesicles could avoid DOX leakage during blood circulation stage and enable fast release at the acidic tumor locations.

3.5. In vitro cytotoxicity evaluation

The cytotoxicity of the polymeric vesicles, the corresponding DOX-loaded vesicles and the free DOX in A549 cells were tested using a CCK-8 assay, which is to detect the number of viable cells in cell proliferation and cytotoxicity assays (Zhuang et al., 2016; Zhao et al., 2020). During the cytotoxicity evaluation, different concentrations of cross-linked vesicle solutions, free DOX solutions and DOX-loaded vesicle solutions were added to the wells with A549 cells and incubated for one day to check the absorbance values. Figure 6(a) shows the relationship of cell viability versus the concentrations of the cross-linked vesicles, and the cell viability showed almost no decrease up to the concentration of 2.0 mg/mL, and thus the cytotoxicity of the cross-linked vesicles was very low. However, after treating A549 cells with free DOX solutions or the DOX-loaded vesicle solutions (DOX concentration of DOX-loaded vesicles was calculated based on the drug loading content), an obvious decline of the cell viability was observed with a DOX concentration in the range of 0.1–1.0 μg/mL, and then the cell viability decreased slowly as the DOX concentration increased, as shown in Figure 6(b). To compare the 50% cellular growth inhibition (IC_{50}) values to A549 cells, IC_{50} was 0.68 μg/mL for the free DOX solution, while for the DOX-loaded vesicle solution, the value was 1.15 μg/mL (the release of DOX from the DOX-loaded vesicles should cause the cytotoxicity). The cytotoxicity of the free DOX could be reduced obviously by encapsulation into the vesicles, which also demonstrates the advantages of applying polymeric vesicles as the drug carriers.

3.6. Intracellular DOX release

Free DOX solution and DOX-loaded vesicle solution (with 0.2 μg/mL concentration of DOX) were used for the investigation of intracellular DOX release. The A549 cells were treated with free DOX solution or DOX-loaded vesicle solution at 37 °C for 24 h, and stained with DAPI (a blue fluorescent dye that can stain the nuclei of the cells) after the cells were fixed with formaldehyde, and then CLSM was applied to do the evaluation. For the cells incubated with free DOX solution, strong blue fluorescence could be seen for the nuclei of A549 cells stained with DAPI, as shown in Figure 7, and weak red fluorescence was also observed, which demonstrated that DOX entered the cell nuclei. While for the A549 cells treated with the DOX-loaded vesicle solution, much stronger red fluorescence was detected, indicating that more DOX-loaded vesicles entered into the cells than did the free DOX, and thus higher cellular uptake capability could be achieved for the DOX-loaded vesicles. This was consistent with the reported result where the entry of free DOX into HeLa cells was slower than that of DOX-loaded nano-objects due to the low solubility of DOX in aqueous solution (Qiu et al., 2016).

4. Conclusions

In this study, the post-encapsulation and release of drugs were examined through the cell-like transmission function of polymeric vesicles. Accordingly, pH-responsive vesicles with cross-linked membranes were fabricated through a post-cross-linking approach, using mPEG-P(DIPEMA-co-GlyMA) vesicles produced through a redox-initiated reversible addition-fragmentation chain transfer dispersion polymerization in ethanol-water mixture. The membrane of the vesicles served as a gate and underwent "open" functionality to enable the anticancer drug DOX to diffuse into the vesicles in an acidic environment, and underwent "closed" functionality to trap the drug in the vesicles under weak alkaline conditions, achieving up to 50% LE and 39% LC. In vitro release of the DOX-loaded vesicles in the aqueous buffer solutions was much faster at pH = 5.0 than at pH = 6.5. The polymeric vesicles caused virtually negligible cytotoxicity to A549 cells up to a concentration of 2.0 mg/mL. The IC_{50} of DOX-loaded vesicles was higher than that of the free DOX. The intracellular DOX release study indicated higher cellular uptake capability for DOX-loaded vesicles than that of free DOX. Therefore, preparation of the pH-responsive vesicles with cross-linked membranes demonstrated a potential method for anticancer drug delivery application.

Disclosure statement

No potential conflict of interest was reported by the authors.

Data availability statement

The data of this study are available from the corresponding author upon reasonable request.

Funding

The authors acknowledge the financial support received from the Natural Science Foundation of Hebei Province (H2021302001) and the Hebei Academy of Sciences (22703).

References

Bories-Azeau X, Armes SP, van den Haak HJW. (2004). Facile synthesis of zwitterionic diblock copolymers without protecting group chemistry. Macromolecules 37:1–11.

Che H, van Hest JCM. (2016). Stimuli-responsive polymersomes and nanoreactors. J Mater Chem B 4:4632–47.

Chen W, Meng FH, Cheng R, Zhong ZY. (2010). pH-sensitive degradable polymersomes for triggered release of anticancer drugs: a comparative study with micelles. J Control Release 142:40–6.

Colley HE, Hearnden V, Avila-Olias M, Cecchin D, Canton I, Madsen J, MacNeil S, Warren N, Hu K, McKeating JA, Armes SP, Murdoch C, Thornhill MH, Battaglia G. (2014). Polymersome-mediated delivery of combination anticancer therapy to head and neck cancer cells: 2D and 3D in vitro evaluation. Mol Pharm 11:1176–88.

Dai XC, Yu LL, Zhang YX, Zhang L, Tan JB. (2019). Polymerization-induced self-assembly via RAFT-mediated emulsion polymerization of methacrylic monomers. Macromolecules 52:7468–76.

Deane OJ, Musa OM, Fernyhough A, Armes SP. (2020). Synthesis and characterization of waterborne pyrrolidone functional diblock copolymer nanoparticles prepared via surfactant-free RAFT emulsion polymerization. Macromolecules 53:1422–34.

Du Y, Jia S, Chen Y, Zhang L, Tan JB. (2021). Type I photoinitiator-functionalized block copolymer nanoparticles prepared by RAFT-mediated polymerization-induced self-assembly. ACS Macro Lett 10:297–306.

Feng A, Yuan J. (2014). Smart nanocontainers: progress on novel stimuli-responsive polymer vesicles. Macromol Rapid Commun 35:767–79.

Fox ME, Szoka FC, Frechet JM. (2009). Soluble polymer carriers for the treatment of cancer: the importance of molecular architecture. Acc Chem Res 42:1141–51.

Gao C, Wang Y, Zhu WP, Shen ZQ. (2014). Resorcinarene-centered amphiphilic star-block copolymers: synthesis, micellization and controlled drug release. Chin J Polym Sci 32:1431–41.

Gu Y, Zhao J, Liu Q, Zhou N, Zhang Z, Zhu X. (2014). Zero-valent iron (Fe(0)) mediated RAFT miniemulsion polymerization: a facile approach for the fabrication of Fe(0)-encapsulated polymeric nanoparticles. Polym Chem 5:4215–8.

Gu Y, Zhao J, Liu Q, Pan X, Zhang W, Zhang Z, Zhu X. (2015). Zero valent metal/RAFT agent mediated CRP of functional monomers at room temperature: a promising catalyst system for CRP. Polym Chem 6:359–63.

Hu XL, Tian J, Liu T, Zhang GY, Liu SY. (2013). Photo-triggered release of caged camptothecin prodrugs from dually responsive shell cross-linked micelles. Macromolecules 46:6243–56.

Hu XL, Zhai SD, Liu GH, Xing D, Liang HJ, Liu SY. (2018). Concurrent drug unplugging and permeabilization of polyprodrug-gated cross-linked vesicles for cancer combination chemotherapy. Adv Mater 30:1706307.

Hu XL, Zhang YG, Xie ZG, Jing XB, Bellotti A, Gu Z. (2017). Stimuli-responsive polymersomes for biomedical applications. Biomacromolecules 18:649–73.

Kamaly N, Yameen B, Wu J, Farokhzad OC. (2016). Degradable controlled-release polymers and polymeric nanoparticles: mechanisms of controlling drug release. Chem Rev 116:2602–63.

Karagoz B, Esser L, Duong HT, Basuki JS, Boyer C, Davis TP. (2014). Polymerization-induced self-assembly (PISA)-control over the morphology of nanoparticles for drug delivery applications. Polym Chem 5:350–5.

Kim BS, Chuanoi S, Suma T, Anraku Y, Hayashi K, Naito M, Kim HJ, Kwon IC, Miyata K, Kishimura A, Kataoka K. (2019). Self-assembly of siRNA/PEG-b-catiomer at integer molar ratio into 100 nm-sized vesicular polyion complexes (siRNAsomes) for RNAi and codelivery of cargo macromolecules. J Am Chem Soc 141:3699–709.

Lee JS, Feijen J. (2012). Polymersomes for drug delivery: design, formation and characterization. J Control Release 161:473–83.

Li X, Yang WJ, Zou Y, Meng FH, Deng C, Zhong ZY. (2015). Efficacious delivery of protein drugs to prostate cancer cells by PSMA-targeted pH-responsive chimaeric polymersomes. J Control Release 220:704–14.

Liu X, Formanek P, Voit B, Appelhans D. (2017). Functional cellular mimics for the spatiotemporal control of multiple enzymatic cascade reactions. Angew Chem 129:16451–6.

Liu Z, Lv Y, An ZS. (2017). Enzymatic cascade catalysis for the synthesis of multiblock and ultrahighmolecular-weight polymers with oxygen tolerance. Angew Chem Int Ed 56:13852–6.

Liu S, Maheshwari R, Kiick KL. (2009). Polymer-based therapeutics. Macromolecules 42:3–13.

Liu GY, Qiu Q, Shen WQ, An ZS. (2011). Aqueous dispersion polymerization of 2-methoxyethyl acrylate for the synthesis of biocompatible nanoparticles using a hydrophilic RAFT polymer and a redox initiator. Macromolecules 44:5237–45.

Liu GH, Tan JJ, Cen J, Zhang GY, Hu JM, Liu SY. (2022). Oscillating the local milieu of polymersome interiors via single input-regulated bilayer crosslinking and permeability tuning. Nat Commun 13:585.

Li Hz, Xu W, Li F, Zeng R, Zhang XM, Wang XW, Zhao SJ, Weng J, Li Z, Sun LP. (2022). Amplification of anticancer efficacy by co-delivery of doxorubicin and lonidamine with extracellular vesicles. Drug Deliv 29:192–202.

Lomas H, Canton I, MacNeil S, Du JZ, Armes SP, Ryan AJ, Lewis AL, Battaglia G. (2007). Biomimetic pH sensitive polymersomes for efficient DNA encapsulation and delivery. Adv Mater 19:4238–43.

Lv Y, Liu Z, Zhu A, An ZS. (2017). Glucose oxidase deoxygenation-redox initiation for RAFT polymerization in air. J Polym Sci Part A: Polym Chem 55:164–74.

Moreno S, Voit B, Gaitzsch J. (2021). The chemistry of cross-linked polymeric vesicles and their functionalization towards biocatalytic nanoreactors. Colloid Polym Sci 299:309–24.

Park M, Kim K, Mohanty AK, Cho HY, Lee H, Kang Y, Seo B, Lee W, Jeon HB, Paik HJ. (2020). Redox-initiated reversible addition-fragmentation chain transfer (RAFT) miniemulsion polymerization of styrene using PPEGMA-based macro-RAFT agent. Macromol Rapid Commun 41:2000399.

Peer D, Karp JM, Hong S, Farokhzad OC, Margalit R, Langer R. (2007). Nanocarriers as an emerging platform for cancer therapy. Nat Nanotechnol 2:751–60.

Penfold NJW, Whatley JR, Armes SP. (2019). Thermoreversible block copolymer worm gels using binary mixtures of PEG stabilizer blocks. Macromolecules 52:1653–62.

Qiu L, Xu CR, Zhong F, Hong CY, Pan CY. (2016). Fabrication of functional nano-objects through RAFT dispersion polymerization and influences of morphology on drug delivery. ACS Appl Mater Interfaces 8:18347–59.

Sztandera K, Gorzkiewicz M, Wang X, Boye S, Appelhans D, Klajnert-Maculewicz B. (2022). pH-stable polymersome as nanocarrier for post-loaded rose bengal in photodynamic therapy. Colloids Surf B Biointerfaces 217:112662.

Tan JB, Zhang X, Liu D, Bai Y, Huang C, Li X, Zhang L. (2017). Facile preparation of CO_2-responsive polymer nano-objects via aqueous photoinitiated polymerization-induced self-assembly (photo-PISA). Macromol Rapid Commun 38:1600508.

Tenchov R, Bird R, Curtze AE, Zhou QQ. (2021). Lipid nanoparticles-from liposomes to mRNA vaccine delivery, a landscape of research diversity and advancement. ACS Nano 15:16982–7015.

Thambi T, Park JH, Lee DS. (2016). Stimuli-responsive polymersomes for cancer therapy. Biomater Sci 4:55–69.

Tian XY, Ding JJ, Zhang B, Qiu F, Zhuang XD, Chen Y. (2018). Recent advances in RAFT polymerization: novel initiation mechanisms and optoelectronic applications. Polymers 10:318.

Wang XR, Hu JM, Liu GH, Tian J, Wang HJ, Gong M, Liu SY. (2015). Reversibly switching bilayer permeability and release modules of photochromic polymersomes stabilized by cooperative noncovalent interactions. J Am Chem Soc 137:15262–75.

Warren NJ, Armes SP. (2014). Polymerization-induced self-assembly of block copolymer nanoobjects via RAFT aqueous dispersion polymerization. J Am Chem Soc 136:10174–85.

Xu XF, Pan CY, Zhang WJ, Hong CY. (2019). Polymerization-induced self-assembly generating vesicles with adjustable pH-responsive release performance. Macromolecules 52:1965–75.

Yao CZ, Li YM, Wang ZX, Song CZ, Hu XL, Liu SY. (2020). Cytosolic NQO1 enzyme-activated near-infrared fluorescence imaging and photodynamic therapy with polymeric vesicles. ACS Nano 14:1919–35.

Yu SY, Azzam T, Rouiller I, Eisenberg A. (2009). "Breathing" vesicles. J Am Chem Soc 131:10557–66.

Yu WQ, Liu R, Zhou Y, Gao HL. (2020). Size-tunable strategies for a tumor targeted drug delivery system. ACS Cent Sci 6:100–16.

Zhang WJ, Hong CY, Pan CY. (2016). Fabrication of reductive-responsive prodrug nanoparticles with superior structural stability by polymerization-induced self-assembly and functional nanoscopic platform for drug delivery. Biomacromolecules 17:2992–9.

Zhang WJ, Hong CY, Pan CY. (2017). Artificially smart vesicles with superior structural stability: fabrication, characterizations, and transmembrane traffic. ACS Appl Mater Interfaces 9:15086–95.

Zhang WJ, Hong CY, Pan CY. (2017). Efficient fabrication of photosensitive polymeric nano-objects via an ingenious formulation of RAFT

dispersion polymerization and their application for drug delivery. Biomacromolecules 18:1210–7.

Zhang F, Niu YL, Li YT, Yao Q, Chen XQ, Zhou HJ, Zhou MM, Xiao JJ. (2021). Fabrication and characterization of structurally stable pH-responsive polymeric vesicles by polymerization-induced self-assembly. RSC Adv 11:29042–51.

Zhao M, Ma W, Ma CN. (2020). Circ_0067934 promotes non-small cell lung cancer development by regulating miR-1182/KLF8 axis and activating Wnt/β-catenin pathway. Biomed Pharmacother 129:110461.

Zhu HS, Geng QR, Chen WQ, Zhu YQ, Chen J, Du JZ. (2013). Antibacterial high-genus polymer vesicle as an "armed" drug carrier. J Mater Chem B 1:5496–504.

Zhu AQ, Lv XQ, Shen LL, Zhang BH, An ZS. (2017). Polymerization-induced cooperative assembly of block copolymer and homopolymer via RAFT dispersion polymerization. ACS Macro Lett 6:304–9.

Zhuang XB, Qiao TK, Xu GX, Yuan SJ, Zhang Q, Chen X. (2016). Combination of nadroparin with radiotherapy results in powerful synergistic antitumor effects in lung adenocarcinoma A549 cells. Oncol Rep 36:2200–6.